

ADAPTIVE TRACTION CONTROL FOR NON-RIGID TIRE-WHEEL SYSTEMS

John Adcox

Clemson University – International Center for
Automotive Research
4 Research Dr., CGEC,
Greenville, SC, 29607, USA
jadcox@g.clemson.edu

Beshah Ayalew

Clemson University – International Center for
Automotive Research
4 Research Dr., CGEC,
Greenville, SC, 29607, USA
beshah@clemson.edu

ABSTRACT

The designs of commercial Anti-Lock Braking Systems often rely on assumptions of a torsionally rigid tire-wheel system. However, variations in tire/wheel technologies have resulted in lower torsional stiffnesses that cannot be captured well using these rigid wheel assumptions. This paper presents an adaptive nonlinear controller based on a model that incorporates sidewall flexibility, and transient & hysteretic tread-ground friction effects. The sidewall stiffness and damping and as well as tread parameters are assumed to be unknown and subsequently estimated through a set of gradient-based adaptation laws. A virtual damper is introduced via a backstepping controller design to address difficulties associated with tires with low torsional damping.

NOMENCLATURE

- θ_r, ω_r – Rotational Deflection & Velocity of the Ring
- θ_w, ω_w – Rotational Deflection & Velocity of the Wheel
- K_t – Torsional Stiffness of the Wheel/Ring
- C_t – Torsional Damping of the Wheel/Ring
- J_w – Wheel Inertia
- J_r – Ring Inertia
- m_v – Vehicle Mass
- R_r – Ring Radius
- R_w – Wheel Radius
- T_b – Braking Torque on the Wheel
- F_t – Frictional Ground Force at the Ring
- F_z – Vertical Load on Tire
- V – Vehicle Velocity
- V_r – Relative Sliding Velocity
- V_s – Stribeck Relative Velocity
- z – Tread Deflection
- $g(V_r)$ – Friction Coefficient Curve
- μ_c – Coulomb Friction

- μ_s – Sliding Friction
- α – Friction Curve Shaping Factor

1. INTRODUCTION

Anti-lock braking (ABS) control algorithms are commonly constructed based on simplified rigid wheel assumptions and primarily focus on accommodating various tire/ground friction surfaces. Advances in tire/wheel technology have produced some tires with significantly lower torsional stiffnesses. This includes airless tires and run-flat tires. In the presence of tire torsional flexibility, there is a distinction between the behavior of the wheel/hub and tread-belt during a hard braking event. Since most, if not all, traction/ABS controllers are based on rigid wheel assumptions and use wheel/hub speed sensors as the main means of feedback, one can expect sub-optimal performance of such controllers when used with torsionally flexible tires.

Various tire models have been developed in order to better approximate the transient dynamics of a tire [1-4]. And multiple authors [5-8] have modeled and simulated commercial ABS control structures that are combined with these various flexible tire models in order to see their effect on braking performance. These works recognize that there is an interaction between the ABS controller and the tire’s torsional dynamics. In our previous work [9], an investigation was conducted on the interactions of tire/wheel designs with the workings of a typical commercial ABS control system. This research showed that a decrease in the tire torsional stiffness can have a drastic impact on the vehicle’s stopping distance.

In recent years, there has been an increased interest in adaptive traction control systems that use dynamic friction models in order to estimate the flexible tread parameters and subsequently calculate a desired slip ratio [10-13]. One of the

original papers to take this approach was by Canudas-de-Wit, et al [10] in which they utilized the LuGre friction model and assumed that all of the tire tread parameters were known except for the friction curve. Variation of the friction curve with road surfaces was taken into account by introducing a gain θ on the friction function that was interpreted as the coefficient of road adhesion. A gradient-type adaptation law was then introduced to estimate this gain during the maneuver. The authors designed a controller to track a desired slip ratio based on an estimation of the maximum friction coefficient at the current vehicle velocity.

The above paper, along with Yi, et al [14], also implemented an observer to estimate velocity and the internal states using only the wheel angular velocity measurement. In [14], the work of Canudas-De-Wit et al was expanded to show that the state estimations guaranteed underestimation of the maximum friction coefficient when the correct initial conditions were chosen. However, the utilization of only wheel angular velocity resulted in an estimator that was slow to converge due to a lack of persistent excitation, a problem common with most adaptive traction controllers. In order to improve the convergence rate, Alvarez, et al [12] proposed an adaptive control law that used both wheel angular velocity and vehicle longitudinal acceleration to estimate the states and tread parameters.

Even though in the past few years there has been an increase in the amount of research on traction/ABS controllers and dynamic friction models, there still appears to be no investigation on including the tire's torsional dynamics into the controller design. The objective of this paper is to expand upon the work of Alvarez, et al. [12] to include and adapt to the tire's sidewall parameters. This paper will focus on the case where both the tire sidewall and tread parameters are unknown. It has been assumed that the vehicle velocity and the friction function are known based on extensive work completed in this area [11-16]. In addition, this paper systematically constructs a virtual damper via backstepping techniques [17] to devise a nonlinear adaptive controller that accommodate tires with low torsional damping.

The rest of the paper is organized as follows. Section 2 describes the system model which incorporates a torsionally flexible tire model and the Average Lumped Parameter LuGre dynamic friction model. Section 3 introduces the parameter estimators and state observers that feed the estimated states into the controller. In Section 4, a nonlinear traction controller will be introduced that tracks an estimated desired slip ratio. In Section 5, the stability analysis of the closed-loop system will be presented. Simulation results of the closed-loop system will be presented in Section 6. The results and conclusions, along with areas for future work, are then summarized in Section 7.

2. TORSIONALLY FLEXIBLE TIRE MODEL

The tire/wheel model that is used throughout this paper only includes the torsional deflection of the sidewall, as this is

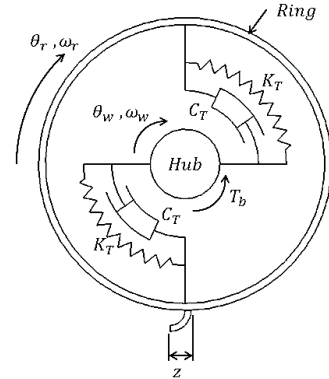


FIGURE 1: HUB/TIRE MODEL

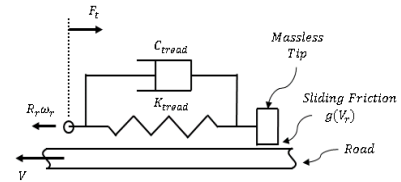


FIGURE 2: SCHEMATIC FOR THE LUGRE FRICTION MODEL

considered to be the dominant effect of the tire/wheel system to braking inputs. The two-inertia model representing the ring and hub is shown in Figure 1. The sidewall's torsional stiffness and damping coefficient are denoted by K_T and C_T , respectively.

Since this paper sets out to account for the dynamic behavior of the tire/wheel system, conventional steady-state Pacejka type (μ -slip) curves are no longer considered sufficient. Instead, a dynamic tread-deflection friction model is incorporated through the Average Lumped Parameter LuGre friction model detailed in [18] and also discussed in [2, 10, 11, 19-21]. In this model, instead of the Pacejka friction curves, the input to the model represents the actual friction coefficient as a function of sliding velocity between the tread material and the road surface. The schematic for this model is shown in Figure 2, where K_{tread} and C_{tread} are stiffness and damping coefficients appearing in the LuGre model [22]. Considering a quarter vehicle model along with the above tire/wheel and tread/ground friction model, the system equations reduce to the following:

$$J_w * \frac{d\omega_w}{dt} = K_t(\theta_r - \theta_w) + C_t(\omega_r - \omega_w) - T_b \quad (1)$$

$$J_r * \frac{d\omega_r}{dt} = F_t R_r - K_t(\theta_r - \theta_w) - C_t(\omega_r - \omega_w) \quad (2)$$

$$\frac{m_v}{4} * \frac{dV}{dt} = -F_t \quad (3)$$

$$F_t = F_z(K_{tread}z + C_{tread}\dot{z}) \quad (4)$$

$$V_r = V - R_r * \omega_r \quad (5)$$

$$\dot{z} = V_r - \frac{K_{tread}|V_r|}{g(V_r)}z - k|\omega_r|R_r z \quad (6)$$

$$g(V_r) = \mu_c + (\mu_s - \mu_c)e^{-|V_r/v_s|^\alpha} \quad (7)$$

where, J_w and J_r designate the hub/wheel and ring inertias, T_b designates the braking torque, and F_t designates the ground force. Equation (3) gives the longitudinal braking dynamics of the quarter vehicle, where aerodynamic and rolling resistance contributions have been neglected. Equations (4)-(7) represent the LuGre friction model. A ‘Stribeck’ friction curve has been extrapolated from experimental data where the static (μ_s) and kinetic (μ_c) coefficients of friction are 0.75 and 0.4, respectively, and the shaping factor (α) has been determined as 0.75. The torsional stiffness of the tire used in the simulations has been determined based on experimental measurements to be $K_T = 7616 [Nm/rad.]$ and is representative of a low torsional stiffness tire (For comparison, $K_T \approx 15000 \rightarrow 25000 [Nm/rad.]$ for a standard “rigid” tire). The rest of system and vehicle parameters used for analysis are listed in the Appendix.

3. PARAMETER AND STATE ESTIMATION

In this section, the parameter adaptation laws are formulated. The following parameters are assumed unknown: K_{tread} , C_{tread} , K_t , C_t and J_w .¹ Rearranging Equation (3) and combining with Equations (1), (2), and (5), we have:

$$\frac{dV_r}{dt} = -(g + a) * \mu + \frac{R_r}{J_r} (J_w \dot{\omega}_w + T_b) \quad (8)$$

where, g is acceleration due to gravity, $\mu = F_t/F_z$ is the coefficient of friction, and $a = (R_r^2 m_v g)/(4 * J_r)$. Then, using Equation (6) in Equation (4) and rearranging to isolate the unknown parameters K_{tread} and C_{tread} gives:

$$\mu = K_{tread} z + C_{tread} (V_r - k|\omega_r|R_r z) - \sigma_3 f(V_r) z \quad (9)$$

where, $f(V_r) = |V_r|/g(V_r)$, and $\sigma_3 = K_{tread} * C_{tread}$. This last additional parameter is introduced to put equation (9) in regressor form (linear in unknown parameters). Assuming that μ , V^2 , and ω_w can be measured, the following gradient-based adaptive law can be constructed:

$$\dot{\mu} = [z \quad (V_r - k|\omega_r|R_r z) \quad -f(V_r) z] * [K_{tread} \quad C_{tread} \quad \sigma_3]^T = U_1 \Sigma_1 \quad (10)$$

$$\dot{\tilde{\mu}} = \hat{U}_1 \hat{\Sigma}_1 - U_1 \Sigma_1 = \hat{U}_1 \hat{\Sigma}_1 - \mu \quad (11)$$

¹ A limitation of this scheme is the assumption that J_r is known. Further work needs to be completed to include this parameter in the adaptation laws.

² A significant amount of research has been conducted on the estimation of the friction coefficient and vehicle velocity. These variables are assumed known in this work.

$$\dot{\hat{\Sigma}}_1 = -\Gamma_1 \hat{U}_1^T \tilde{\mu} \quad \text{where,} \quad \Gamma_1 = \text{diag}(\gamma_0, \gamma_1, \gamma_3) > 0 \quad (12)$$

where, the notation $\hat{\cdot}$ represents an estimated state or parameter; Γ_1 is a positive diagonal matrix of adaptation gains and $\hat{U}_1 = [\hat{z} \quad (\hat{V}_r - k|\hat{\omega}_r|R_r \hat{z}) \quad -f(\hat{V}_r) \hat{z}]$ is the regressor matrix evaluated at the estimated states.

Estimation of the sidewall torsional parameters can also be made by following a similar procedure. We assume that T_b is measurable (can be inferred from brake pressure). By rearranging Equation (1) into a regressor form and solving for T_b :

$$T_b = [(\theta_r - \theta_w) \quad (\omega_r - \omega_w) \quad -\dot{\omega}_w] * [K_t \quad C_t \quad J_w]^T = U_2 \Sigma_2 \quad (13)$$

$$\dot{\tilde{T}} = \hat{U}_2 \hat{\Sigma}_2 - U_2 \Sigma_2 = \hat{U}_2 \hat{\Sigma}_2 - T_b \quad (14)$$

where, $\hat{U}_2 = [(\hat{\theta}_r - \theta_w) \quad (\hat{\omega}_r - \omega_w) \quad -\dot{\omega}_w]$ is the regressor matrix evaluated at the estimated states. The following gradient-based adaptation law can be constructed:

$$\dot{\hat{\Sigma}}_2 = -\Gamma_2 \hat{U}_2^T \tilde{T} \quad \text{where,} \quad \Gamma_2 = \text{diag}(\gamma_4, \gamma_5, \gamma_6) > 0 \quad (15)$$

The gradient-based adaptation laws can be replaced with least-squares estimators and techniques such as parameter projection and dead-zones can be used add robustness to the adaptation. However, for the investigations in this paper the above formulation was found sufficient.

These parameter estimates are then used to construct an estimated plant, of the same structure as Equations (1)-(7), from which the unmeasured state estimates $\hat{\theta}_r$, $\hat{\omega}_r$, and \hat{z} are obtained through an open-loop observer. See Figure 5 for a schematic. Note that, due to the parameter adaptation scheme and the inability to separate the estimated states from the estimated parameters, it is not trivial to introduce a closed-loop observer. Further work is currently being completed by the authors to incorporate a closed-loop observer into the system.

4. NONLINEAR TRACTION CONTROLLER

The design of the controller is approached in two parts. First, it is treated as a ring slip-tracking problem. Then, additional virtual damping terms are systematically included to overcome oscillations from low tire damping.

For a traction controller, it is desirable to track the ring slip ratio that corresponds to the peak friction force in order to minimize stopping distance. This desired slip ratio λ_m can be estimated based upon a pseudo-static computation of the LuGre friction model at a given velocity and assuming a uniformly

distributed loading with a rectangular contact patch. Detailed derivations of similar equations which are based on the rigid sidewall model can be found in [10] and [11], where ω_r is replaced with the rigid wheel rotational velocity. The computation used in this paper proceeds as follows:

$$\hat{F}_{ss} = \text{sgn}(V_r) F_z g(V_r) \left(1 + 2\hat{\gamma} \frac{g(V_r)}{\hat{R}_{tread} L |\eta|} \left(e^{\frac{\hat{R}_{tread} L |\eta|}{2g(V_r)}} - 1 \right) \right) \quad (16)$$

$$\hat{\gamma} = 1 - \frac{\hat{C}_{tread} |V_r|}{g(V_r)} \quad (17)$$

$$\eta = \frac{V_r}{R_r \omega_r} = \frac{\lambda_r}{1 - \lambda_r} \quad (18)$$

$$\lambda_r = \frac{V - R_r \omega_r}{V} = \frac{V_r}{V} \quad (19)$$

where, L is the contact patch length. An estimate of the desired slip ratio λ_m can then be obtained by numerically searching Equation (16) for its maximum by varying λ_r [11, 12, 14],

$$\hat{\lambda}_m = \underset{\lambda_r}{\text{argmax}} \{F_{ss}(\lambda_r, V_r, \hat{\Sigma})\} \quad (20)$$

Then, recognizing that $\hat{\omega}_r$ and $\hat{\theta}_r$ are only estimated states, Equation (2) can be rewritten as:

$$J_r * \frac{d\hat{\omega}_r}{dt} = F_t R_r - \hat{R}_t(\hat{\theta}_r - \theta_w) - \hat{C}_t(\hat{\omega}_r - \omega_w) \quad (21)$$

Combining (14) & (21),

$$\frac{d\hat{\omega}_r}{dt} = \frac{1}{J_r} \left[F_t R_r - \tilde{T} - \hat{J}_w * \frac{d\omega_w}{dt} - T_{b1} \right] \quad (22)$$

where T_{b1} is the braking torque applied corresponding to the ring slip-tracking problem. Defining the tracking error dynamics as:

$$e = \hat{\omega}_r - \hat{Y}_d \Rightarrow \dot{e} = \frac{d\hat{\omega}_r}{dt} - \dot{\hat{Y}}_d \quad (23)$$

where, $\hat{Y}_d = \frac{V}{R} * (1 - \hat{\lambda}_m)$ is an estimated desired ring rotational velocity corresponding to the estimated desired slip ratio $\hat{\lambda}_m$. Choosing the following (partial) Lyapunov-like candidate:

$$V = \frac{1}{2} e^2 \quad (24)$$

$$\dot{V} = e \left(\frac{1}{J_r} \left[F_t R_r - \tilde{T} - \hat{J}_w \frac{d\omega_w}{dt} - T_{b1} \right] - \dot{\hat{Y}}_d \right)$$

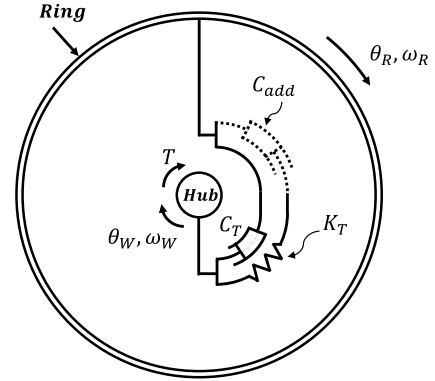


FIGURE 3: HUB/TIRE MODEL EMULATED BY CONTROLLER

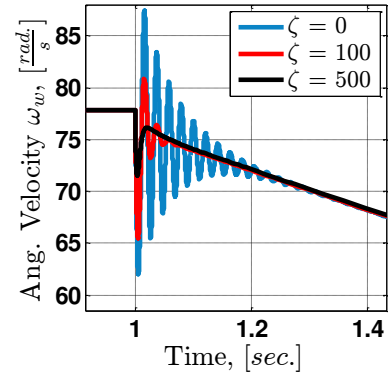


FIGURE 4: RESPONSE OF HUB/TIRE MODEL EMULATED BY CONTROLLER

If we set the controller as:

$$T_{b1} = F_t R_r - \tilde{T} - \hat{J}_w * \frac{d\omega_w}{dt} - J_r \dot{\hat{Y}}_d + J_r c_1 e \quad (25)$$

where, c_1 is a positive controller gain, then, $\dot{V} = -c_1 e^2$, which is negative semi-definite. This shall be used in the stability analysis of the next section.

While this controller will track the desired slip ratio and accounts for tire flexibilities, observations have shown that the low torsional damping of the tire can result in large initial oscillations of brake torque T_{b1} in the presence of tire/tread parameter estimation errors. In order to address this issue, it has been found that a virtual torsional damper can be simulated through the controller. This virtual damper (C_{add}) can be thought of as added in series between the original torsional spring and the tire ring, as shown in Figure 3. By including this virtual damper the controller can effectively emulate a highly damped system. Note that this damper is not placed in series with the physical damper C_t as this would only result in a further decrease in overall damping. The virtual damper can be systematically constructed into the controller using backstepping techniques and the certainty equivalence principle. Similar examples can be found in [23, 24]. Here, choosing the Lyapunov function candidate:

$$V_1 = \frac{1}{2}J_r\omega_r^2 + \frac{1}{2}K_t(\theta_w - \theta_r)^2 \quad (26)$$

$$\dot{V}_1 = J_r\omega_r \left(\frac{1}{J_r} [-K_t(\theta_r - \theta_w) - C_t(\omega_r - \omega_w)] + K_t(\theta_w - \theta_r)(\omega_w - \omega_r) \right) \quad (27)$$

$$= \omega_r(C_t(\omega_w - \omega_r)) + K_t(\theta_w - \theta_r)\omega_w \quad (28)$$

Let the virtual control $\omega_w = -\omega_D$. Where, ω_D represents the relative velocity of the virtual damper and follows the relation $\omega_D = \phi(T_D)$. Also, $T_D = K_t(\theta_w - \theta_r)$ is the torque in the damper³ and $\phi(*)$ is a function chosen by the designer to have the same sign as its argument⁴, thus making the second term in Equation (28) negative semi-definite. The derivative of the relative velocity ω_D can be found through the following analysis:

$$\begin{aligned} \dot{\omega}_D &= \frac{d\phi(T_D)}{dt} = \frac{d\phi(T_D)}{dT_D} * \dot{T}_D \\ &= \frac{d\phi(T_D)}{dT_D} * (K_t(\omega_w - \omega_r)) \\ &= \zeta * (\omega_w - \omega_r) \end{aligned} \quad (29)$$

where, $\zeta = \frac{d\phi(T_D)}{dT_D} * K_t$ is chosen to be positive. Then, continuing with the backstepping procedure, the following change of variables can be applied:

$$\begin{aligned} \gamma &= \omega_w - (-\omega_D) = \omega_w + \omega_D \\ \dot{\gamma} &= \frac{1}{J_w} (K_t(\theta_r - \theta_w) + C_t(\omega_r - \omega_w) - T_{b2}) + \dot{\omega}_D \end{aligned} \quad (30)$$

Choosing the following Lyapunov candidate:

$$V_2 = \frac{1}{2}J_r\omega_r^2 + \frac{1}{2}K_t(\theta_w - \theta_r)^2 + \frac{1}{2}J_w\gamma^2 + \frac{1}{2}C_t \left(\frac{dT_D}{d\phi(T_D)} \frac{1}{K_t} \right) \omega_D^2 \quad (31)$$

$$\dot{V}_2 = J_r\omega_r\dot{\omega}_r + K_t(\theta_w - \theta_r)(\gamma - \omega_D - \dot{\omega}_r) + J_w\gamma\dot{\gamma} + \omega_D(C_t(\omega_w - \omega_r)) \quad (32)$$

Combining Equations (30) and (32) and simplifying

$$\dot{V}_2 = -\omega_D(K_t(\theta_w - \theta_r)) - C_t(\omega_w - \omega_r)^2 + \gamma(-T_{b2} + J_w\dot{\omega}_D) \quad (33)$$

³ Since the spring and virtual damper are in series and massless, the torque created in the virtual damper is equal to the torque in the physical spring.

⁴ It is desirable to emulate a damper that dissipates energy from the system.

Letting $T_{b2} = J_w\dot{\omega}_D$, Equation (33) becomes

$$\dot{V}_2 = -\omega_D(K_t(\theta_w - \theta_r)) - C_t(\omega_w - \omega_r)^2 \leq 0 \quad (34)$$

Then, utilizing Equation (29) T_{b2} can be placed in its final form:

$$T_{b2} = \zeta * J_w(\omega_w - \omega_r) \quad (35)$$

Figure 4 shows the response of the system for various choices of ζ for a step input in brake torque. It is clear that as ζ is increased the system's response is more representative of a well-damped system. Utilizing Equations (25) and (35) the final combined brake torque is represented as follows:

$$T_b = F_t R_r - \tilde{T} - \hat{J}_w * \frac{d\omega_w}{dt} - J_r \dot{\hat{Y}}_d - J_r c_1 e + \phi_D(\omega_w - \hat{\omega}_r) \quad (36)$$

When this controller is combined with the parameter and state estimation of the previous section, the closed-loop system can be represented as shown in Figure 5.

5. STABILITY ANALYSIS

The stability of the closed-loop system, comprising of the parameter and state estimators and the controller tracking error, can be analyzed by choosing the following Lyapunov function candidate:

$$\begin{aligned} W &= \frac{1}{2}\tilde{z}^2 + \frac{1}{2}\tilde{\omega}_r^2 + \frac{1}{2}e^2 + \frac{1}{2}\tilde{\Sigma}_1^T \Gamma_1^{-1} \tilde{\Sigma}_1 \\ &\quad + \frac{1}{2}\tilde{\Sigma}_2^T \Gamma_2^{-1} \tilde{\Sigma}_2 \Rightarrow \\ \dot{W} &= \tilde{z}\dot{\tilde{z}} + \tilde{\omega}_r\dot{\tilde{\omega}}_r + e\dot{e} + \tilde{\Sigma}_1^T \Gamma_1^{-1} \dot{\tilde{\Sigma}}_1 + \tilde{\Sigma}_2^T \Gamma_2^{-1} \dot{\tilde{\Sigma}}_2 \\ &= \tilde{z}\dot{\tilde{z}} + \tilde{\omega}_r\dot{\tilde{\omega}}_r + e\dot{e} - \tilde{\Sigma}_1^T \tilde{U}_1 [\tilde{U}_1 \tilde{\Sigma}_1 + \tilde{U}_2 \Sigma_1] \\ &\quad - \tilde{\Sigma}_2^T \tilde{U}_2 [\tilde{U}_2 \tilde{\Sigma}_2 + \tilde{U}_2 \Sigma_2] \end{aligned} \quad (37)$$

where, $\tilde{U}_1 = \tilde{U}_{11}\tilde{\omega}_r + \tilde{U}_{12}\tilde{z}$ and $\tilde{U}_2 = \tilde{U}_{21}\tilde{\theta}_r + \tilde{U}_{22}\tilde{\omega}_r$. This leads to:

$$\begin{aligned} \tilde{U}_{11} &= [1 \quad -k|\omega_r|R_r \quad -f(V_r)] \\ \tilde{U}_{12} &= [(\theta_r - \theta_w) \quad (\omega_r - \omega_w) \quad -\dot{\omega}_w] \end{aligned} \quad (38)$$

$$\begin{aligned} \tilde{U}_{21} &= [1 \quad 0 \quad 0] \\ \tilde{U}_{22} &= [0 \quad 1 \quad 0] \end{aligned} \quad (39)$$

$\dot{\tilde{z}}$ is computed as follows:

$$\begin{aligned} \dot{\tilde{z}} &= V_r - K_{tread} f(V_r)z - k|\omega_r|R_r z \\ &\quad - [V_r - \hat{K}_{tread} f(V_r)\hat{z} - k|\hat{\omega}_r|R_r \hat{z}] \\ \xrightarrow{yields} \dot{\tilde{z}} &= -\tilde{\omega}_r R_r [1 - K_{tread} f'(V_r)\hat{z} + kh'(\omega_r)\hat{z}] \\ &\quad - \tilde{z}[K_{tread} f(V_r) + kR_r h(\omega_r)] \end{aligned} \quad (40)$$

$$= -\tilde{\omega}_r A - \tilde{z} B$$

where,

$$f'(V_r) = \frac{df(V_r)}{dV_r} = \frac{1}{\tilde{V}_r} [f(V_r) - f(\tilde{V}_r)] = \frac{-1}{\tilde{\omega}_r R_r} [f(V_r) - f(\tilde{V}_r)] \quad (41)$$

And

$$h(\omega_r) = |\omega_r| \Rightarrow h'(V_r) = \frac{dh(\omega_r)}{d\omega_r} = \frac{1}{\tilde{\omega}_r} [h(\omega_r) - h(\tilde{\omega}_r)] \quad (42)$$

And $\dot{\tilde{\omega}}_r$ is computed as follows:

$$\begin{aligned} \dot{\tilde{\omega}}_r &= \frac{1}{J_r} [F_t R_r - K_t(\theta_r - \theta_w) - C_t(\omega_r - \omega_w)] \\ &\quad - \frac{1}{J_r} [F_t R_r - \hat{K}_t(\hat{\theta}_r - \theta_w) - \hat{C}_t(\hat{\omega}_r - \omega_w)] \\ \xrightarrow{yields} \dot{\tilde{\omega}}_r &= \frac{1}{J_r} [-\tilde{K}_t(\theta_r - \theta_w) - \tilde{C}_t(\omega_r - \omega_w) - \hat{K}_t \tilde{\theta}_r \\ &\quad - \hat{C}_t \tilde{\omega}_r] \end{aligned} \quad (43)$$

Utilizing Equations (38) through (43), Equation (37) can be rewritten in quadratic form as follows:

$$\dot{W} = -[\tilde{\Sigma}_1 \quad \tilde{\Sigma}_2 \quad \tilde{z} \quad \tilde{\theta}_r \quad \tilde{\omega}_r \quad e][M] \begin{bmatrix} \tilde{\Sigma}_1 \\ \tilde{\Sigma}_2 \\ \tilde{z} \\ \tilde{\theta}_r \\ \tilde{\omega}_r \\ e \end{bmatrix} = -\phi^T M \phi \quad (44)$$

where, $\phi = [\tilde{\Sigma}_1 \quad \tilde{\Sigma}_2 \quad \tilde{z} \quad \tilde{\theta}_r \quad \tilde{\omega}_r \quad e]$, and

$$M = \begin{bmatrix} \hat{U}_1^T \hat{U}_1 & 0 & \hat{U}_1^T U_{12} \Sigma_1 & 0 & \hat{U}_1^T U_{11} \Sigma_1 & 0 \\ 0 & \hat{U}_2^T \hat{U}_2 & 0 & \hat{U}_2^T U_{21} \Sigma_2 & \hat{U}_2^T U_{22} \Sigma_2 & 0 \\ 0 & 0 & B & 0 & A & 0 \\ 0 & 0 & 0 & 1 & 0 & 0 \\ 0 & C & 0 & \frac{\hat{K}_T}{J_r} & \frac{\hat{C}_T}{J_r} & 0 \\ 0 & 0 & 0 & 0 & 0 & c_1 \end{bmatrix} \quad (45)$$

where,

$$C = \left[\frac{1}{J_r}(\theta_r - \theta_w) \quad \frac{1}{J_r}(\omega_r - \omega_w) \quad 0 \right]$$

M can be decomposed into a symmetric matrix $M_1 = (M + M^T)/2$, and a skew-symmetric matrix $M_2 = (M - M^T)/2$. For a real matrix M , we have: $-\phi^T M_2 \phi = 0$ due to the properties of a skew-symmetric matrix. And it can be shown, for the matrix M given by Equation (45), that the principle minors of M_1 are all non-negative, and therefore, M_1 is positive semi-definite [25]. Thus,

$$\dot{W} = -\phi^T M_1 \phi \leq 0 \quad (46)$$

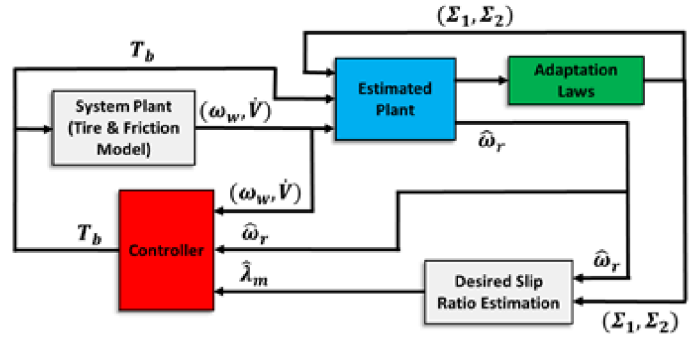


FIGURE 5: SCHEMATIC OF PROPOSED ADAPTIVE CONTROLLER SCHEME

Thus the equilibrium point $[\tilde{\Sigma}_1 \quad \tilde{\Sigma}_2 \quad \tilde{z} \quad \tilde{\theta}_r \quad \tilde{\omega}_r \quad e] = 0$ is stable and the corresponding estimation and tracking errors are bounded. Using Barbalat's Lemma it can be shown that $\lim_{t \rightarrow \infty} e = 0$. However, for guaranteed parameter and state convergence the states are required to be persistently excited.

6. RESULTS AND DISCUSSIONS

This section tests the closed-loop system presented in this paper through simulations. Emergency braking tests are simulated for a quarter-car model of a small passenger vehicle (1068 Kg) with an initial velocity of 80kph, and a low torsional stiffness tire. The vehicle begins the braking event at $t = 0.5$ sec.

In order to establish a baseline, it is sought to evaluate the performance of the traction controller when the controller assumes that the tire sidewall is rigid. This is completed by adopting the controller proposed in [12] and coupling it with the low torsional stiffness tire. The results of these simulation tests are shown in Figures 6 & 7 and highlight the difficulty the controller has in preventing initial oscillations in the ring velocity. Note that the black dotted line V/R represents the vehicle's equivalent rotational velocity. While the adaptation laws still perform very well in the presence of the un-modeled dynamics, the brake torque and subsequently the ring angular velocity are very oscillatory upon initial brake application. These un-modeled dynamics also cause large oscillations in the brake torque and angular velocities later in the event due to the challenges of maintaining a desired slip ratio at low velocities. It should also be noted that there is an increase in the optimal slip ratio as velocity decreases. This trend is consistent with the LuGre model as the peak friction coefficient will actually occur at a fixed sliding velocity (V_r) and not a fixed slip ratio (λ_r).

Figures 8 & 9 show the system response for the adaptive controller proposed in this paper. The system parameters & estimated states are assumed to be unknown prior to the event. In reality it is likely that the adaptation laws have been enabled prior to the hard braking event, thus allowing for a more precise estimate of the system parameters and states. However, by assuming that the parameters and states are unknown prior to the event, a dramatic variation in the system parameters can be represented. Initial estimates of the tire's torsional properties

are assumed to be on the order of a standard tire. These initial parameters are chosen to highlight the most challenging case when an initial estimated tire is significantly stiffer than the actual tire. An example of this scenario may be when there is a sudden loss in tire pressure or immediately following the installation of a new set of tires.

Figure 9 shows the parameter and state estimations for the braking event. The estimated states errors \tilde{z} and $\tilde{\omega}_r$, as well as the estimated tread parameter K_{tread} quickly converge to zero. The remainder of the parameter estimates also begins to converge towards their actual values. However, due to the lack of persistent excitation these parameter estimates are unable to completely converge. This issue is a common problem in adaptive control as the persistence of excitation decreases with an increase in controller performance when the reference trajectory itself is unable to sufficiently excite the states. It should also be realized that, as the oscillations die out, the actual ring velocity will approach that of the measured wheel velocity. This highlights that the tire torsional parameters do not need to completely converge to the true parameters in order to have good performance.

Figure 8 shows the angular velocity trajectories and braking torque for this maneuver. It is important to note that the wheel slip ratio will initially overshoot the optimal ring slip ratio. This is a desirable response as wheel slip ratio does not appear in the tracking error dynamics (Equation (23)) and the controller is taking advantage of the sidewall flexibility in order to build up the ring slip ratio as quickly as possible.

Figures 10 & 11 illustrate the system response when the sidewall parameters are known but the tread parameters remain unknown. During this event the tread parameters are able to very quickly converge to their true values. The angular velocity

responses, shown in Figure 10, also show a very smooth response with almost no oscillations in the ring angular velocity.

Finally, Figures 12 & 13 show the response of the system when the added virtual damper C_{add} is not emulated through the controller. Although the controller is still very successful at tracking the desired ring slip ratio, the braking torque, shown in Figure 12, is very oscillatory and reaches very large positive and negative values. These dramatic oscillations cause the wheel angular velocity ω_w to be oscillatory and even reach negative values. These responses are not realistic, due to limits on the brake hydraulics, and are not desirable. Therefore, to better account for the tire's low torsional damping, it is useful to include a virtual damper through the controller in order to emulate a well-damped system.

CONCLUSION

This paper proposed an adaptive controller that estimates both the tire sidewall and tread parameters & states using a dynamic friction/tread model and a torsionally flexible tire model. The scheme assumes that the vehicle longitudinal velocity, traction force at the ground, wheel speed, and brake torque are measurable. The controller was designed to account for the tire's sidewall flexibility, to track the optimal slip ratio, and included a virtual damper in order to emulate a highly damped system. Closed-loop stability analysis was performed using Lyapunov functions to prove boundedness of the parameter and state errors as well as the convergence of the controller tracking error. Simulation results showed that the controller was able to successfully track the desired slip ratio even when the initial parameters are assumed to be unknown. When the sidewall parameters are known but the tread parameters are not, the adaptive controller scheme showed very

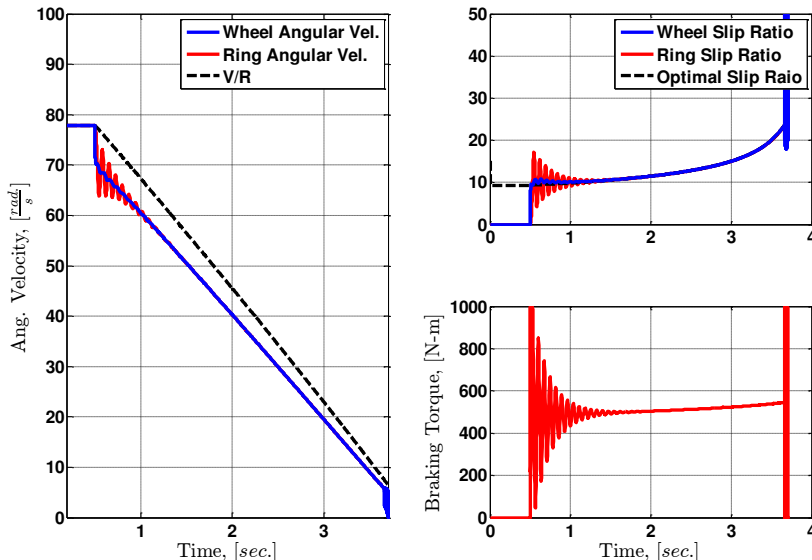


FIGURE 6: BRAKING RESPONSE FOR "RIGID TIRE" BASED ADAPTIVE CONTROLLER

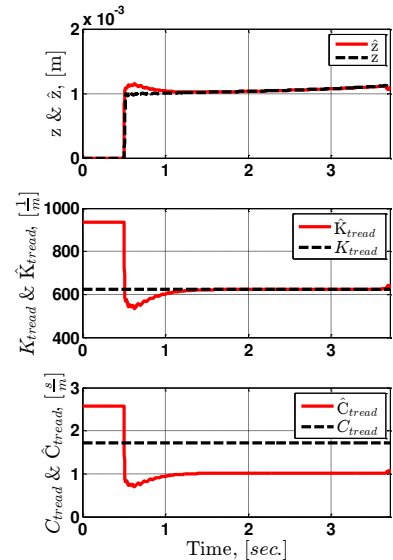


FIGURE 7: PARAMETRIC ESTIMATIONS & ERRORS FOR "RIGID TIRE" BASED CONTROLLER

quick convergence of the tread parameters and states and was able to track the optimal slip ratio with minimal control effort.

Future work will introduce the physical brake hydraulics dynamics. Additional observers and adaptation techniques can

be included to eliminate the requirements of longitudinal velocity measurement and prior knowledge of the friction function.

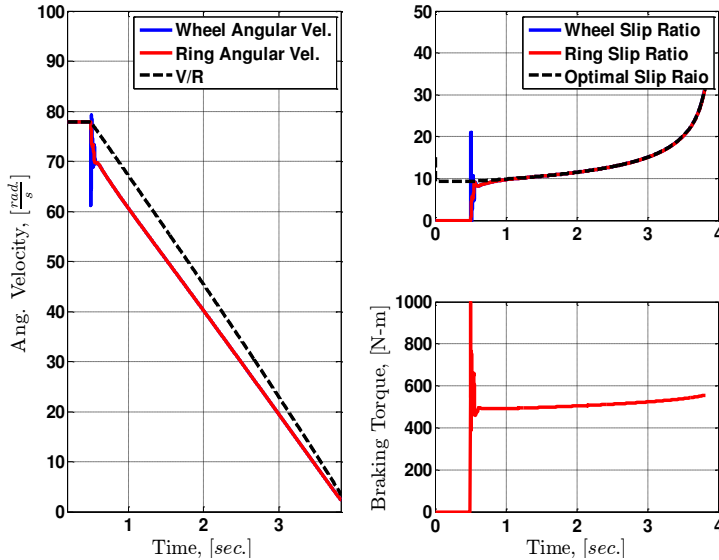


FIGURE 8: BRAKING RESPONSE FOR PROPOSED CONTROLLER (UNKNOWN PARAMETERS)

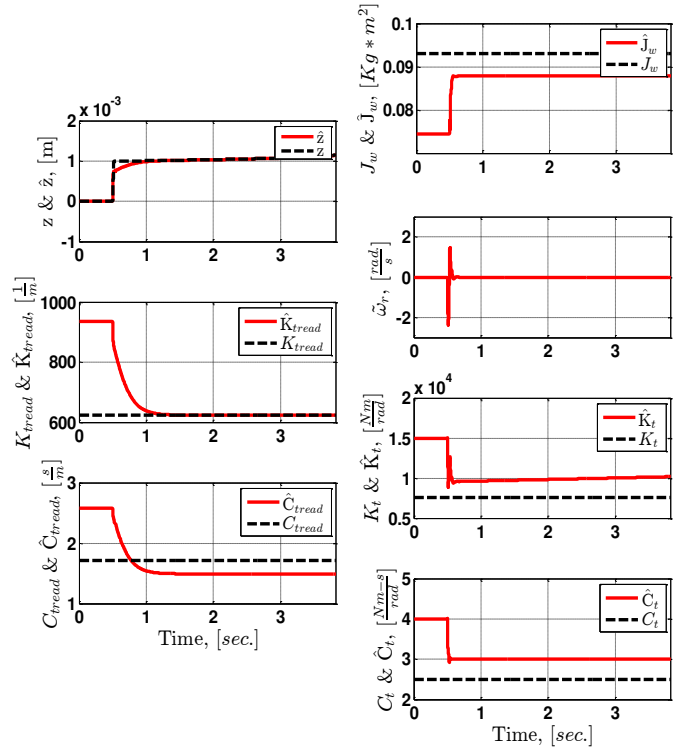


FIGURE 9: PARAMETRIC ESTIMATIONS & ERRORS FOR PROPOSED CONTROLLER (UNKNOWN PARAMETERS)

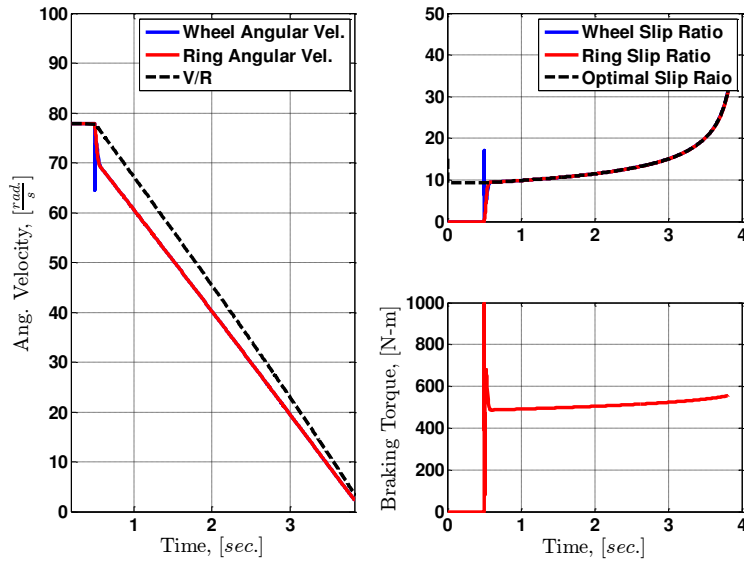


FIGURE 10: BRAKING RESPONSE FOR PROPOSED CONTROLLER (KNOWN TIRE PARAMETERS)

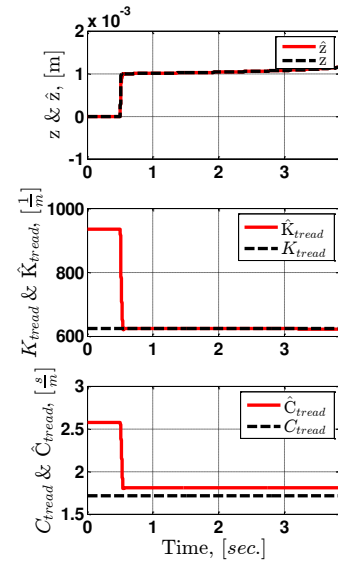


FIGURE 11: PARAMETRIC ESTIMATIONS & ERRORS FOR PROPOSED CONTROLLER (KNOWN TIRE PARAMETERS)

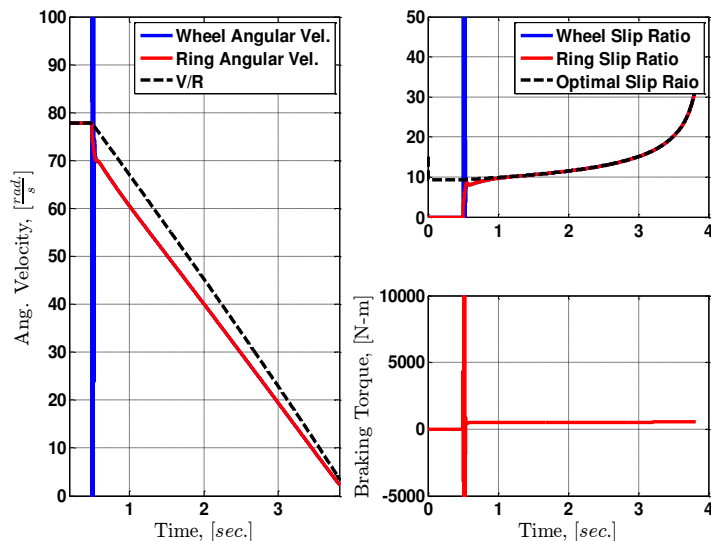


FIGURE 12: BRAKING RESPONSE FOR PROPOSED CONTROLLER (UNKNOWN PARAMETERS & NO VIRTUAL DAMPER)

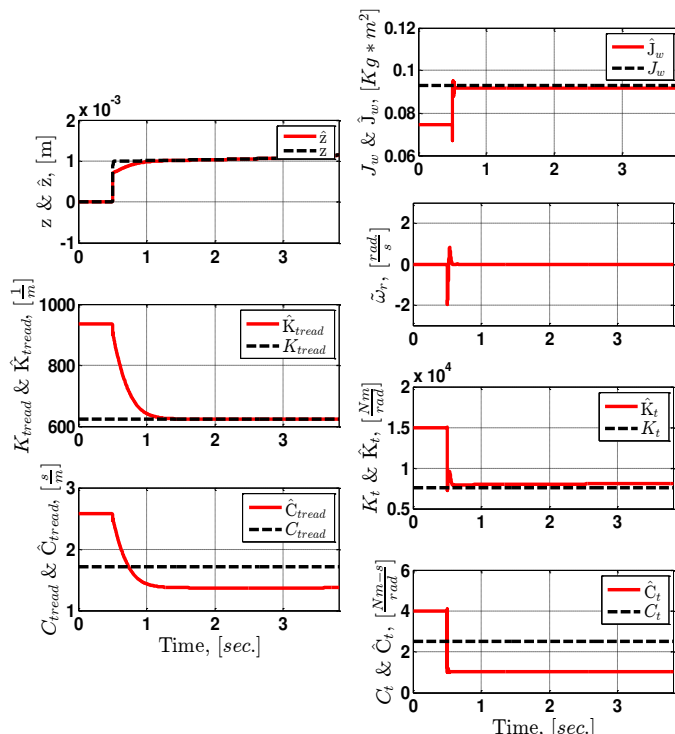


FIGURE 13: PARAMETRIC ESTIMATIONS & ERRORS FOR PROPOSED CONTROLLER (UNKNOWN PARAMETERS & NO VIRTUAL DAMPER)

REFERENCES

- [1] E. Bakker, H. Pacejka, and L. Lidner, "A New Tire Model with an Application in Vehicle Dynamics Studies," 1989.
- [2] C. Canudas-de-Wit, H. Olsson, K. J. Astrom, and P. Lischinsky, "A new model for control of systems with friction," *IEEE Transactions on Automatic Control*, vol. 40, pp. 419-25, 03/ 1995.
- [3] A. Tsiotras and G. Mavros, "Frictional contact behaviour of the tyre: the effect of tread slip on the in-plane structural deformation and stress field development," *Vehicle System Dynamics*, vol. 48, pp. 891-921, 2010/08/01 2009.
- [4] P. W. A. Zegelaar, S. Gong, and H. B. Pacejka, "Tyre models for the study of in-plane dynamics," *Vehicle System Dynamics*, vol. 23, pp. 578-590, 1994.
- [5] F. Braghin and E. Sabbioni, "A Dynamic Tire Model for ABS Maneuver Simulations," *Tire Science & Technology*, vol. 38, pp. 137-54, 06/ 2010.
- [6] J. P. Pauwelussen, L. Gootjes, C. Schroder, K. U. Kohne, S. Jansen, and A. Schmeitz, "Full vehicle ABS braking using the SWIFT rigid ring tyre model," *Control Engineering Practice*, vol. 11, pp. 199-207, 2003.
- [7] K. Z. Rangelov, "SIMULINK Model of a Quarter-Vehicle with an Anti-lock Braking System," Eindhoven University of Technology, 2004.
- [8] S. T. H. Jansen, P. W. A. Zegelaar, and H. B. Pacejka, "The influence of in-plane tyre dynamics on ABS braking of a quarter vehicle model," in *Advanced Vehicle Control (AVEC) 1998, 1998*, Netherlands, 1999, pp. 249-61.
- [9] J. Adcox, B. Ayalew, T. Rhyne, S. Cron, and M. Knauff, "Interaction of anti-lock braking systems with tire torsional dynamics," *Tire Science and Technology*, vol. 40, pp. 171-185, 2012.
- [10] C. Canudas-de-Wit, P. Tsiotras, E. Velenis, M. Basset, and G. Gissinger, "Dynamic friction models for road/tire longitudinal interaction," *Vehicle System Dynamics*, vol. 39, pp. 189-226, 2003.
- [11] C. Canudas-de-Wit and P. Tsiotras, "Dynamic tire friction models for vehicle traction control," in *Proceedings of the 38th IEEE Conference on Decision and Control*, Piscataway, NJ, USA, 1999, pp. 3746-51.
- [12] L. Alvarez, J. Yi, R. Horowitz, and L. Olmos, "Dynamic friction model-based tire-road friction estimation and emergency braking control," *Transactions of the ASME. Journal of Dynamic Systems, Measurement and Control*, vol. 127, pp. 22-32, 2005.
- [13] J. Yi, L. Alvarez, R. Horowitz, and C. Canudas-de-Wit, "Adaptive emergency braking control using a dynamic tire/road friction model," in *Proceedings of*

the 39th IEEE Conference on Decision and Control, Piscataway, NJ, USA, 2000, pp. 456-61.

- [14] J. Yi, L. Alvarez, X. Claeys, and R. Horowitz, "Emergency braking control with an observer-based dynamic tire/road friction model and wheel angular velocity measurement," *Vehicle System Dynamics*, vol. 39, pp. 81-97, 2003.
- [15] W. Wei-Yen, I. H. Li, C. Ming-Chang, S. Shun-Feng, and H. Shi-Boun, "Dynamic slip-ratio estimation and control of antilock braking systems using an observer-based direct adaptive fuzzy-neural controller," *IEEE Transactions on Industrial Electronics*, vol. 56, pp. 1746-56, 05/ 2009.
- [16] Y. Chen and J. Wang, "Adaptive Vehicle Speed Control With Input Injections for Longitudinal Motion Independent Road Frictional Condition Estimation," *IEEE Transactions on Vehicular Technology*, vol. 60, pp. 839-48, 03/ 2011.
- [17] M. Krstic, I. Kanellakopoulos, and P. Kokotovic, *Nonlinear and Adaptive Control Design*: John Wiley and Sons, 1995.
- [18] E. Velenis, P. Tsiotras, C. Canudas-De-Wit, and M. Sorine, "Dynamic tyre friction models for combined longitudinal and lateral vehicle motion," *Vehicle System Dynamics*, vol. 43, pp. 3-29, 2005.
- [19] K. Johansson and C. Canudas-de-Wit, "Revisiting the LuGre friction model," *IEEE Control Systems Magazine*, vol. 28, pp. 101-14, 2008.
- [20] C. L. Clover and J. E. Bernard, "Longitudinal tire dynamics," *Vehicle System Dynamics*, vol. 29, pp. 231-259, 1998.
- [21] L. Wei, J. Medanic, and R. Ruhl, "Analytical dynamic tire model," *Vehicle System Dynamics*, vol. 46, pp. 197-227, 03/ 2008.
- [22] J. Deur, V. Ivanovic, D. Pavkovic, D. Hrovat, J. Asgari, M. Troulis, *et al.*, "Experimental analysis and modelling of longitudinal tyre friction dynamics for abrupt transients," *Vehicle System Dynamics*, vol. 43, pp. 525-39, 2005.
- [23] T.-J. Yeh, "Backstepping control in the physical domain," in *Proceedings of the 1999 American Control Conference, 2-4 June 1999*, Piscataway, NJ, USA, 1999, pp. 24-8.
- [24] T. J. Yeh, "Backstepping control in the physical domain," *Journal of the Franklin Institute*, vol. 338, pp. 455-479, 7// 2001.
- [25] D. S. Bernstein, *Matrix Mathematics: Theory, Facts, And Formulas With Application To Linear Systems Theory*. Princeton, New Jersey: Princeton University Press, 2005.

APPENDIX

	Parameters
K_T [Nm/rad.]	7616
C_T [Nm · s/rad.]	2.5
J_w [Kg · m ²]	0.093
J_r [Kg · m ²]	1
K_{tread} [1/m]	623
C_{tread} [s/m]	1.72
R_r [m]	0.154
m_v [Kg]	1068
μ_c	0.75
μ_s	0.4
V_s [m/s]	10
α	0.75